SUPPLEMENTARY FIGURES

Endothelial Piezo1 mediates mechano-feedback control of brain blood flow

Xin Rui Lim[#,1,2], Mohammad M. Abd-Alhaseeb[#,1,2], Michael Ippolito[1,2], Masayo Koide[1,2], Amanda J. Senatore[1,2], Curtis Plante[1,2], Ashwini Hariharan[3,4], Nick Weir[3,4], Thomas A. Longden[3,4], Kathryn A. Laprade[5], James M. Stafford[5], Dorothea Ziemens[6,7], Markus Schwaninger[6,7], Jan Wenzel[6,7], Dmitry D. Postnov[8], Osama F. Harraz*[,1,2]

[1] Department of Pharmacology, Larner College of Medicine, University of Vermont, Burlington, VT, USA; [2] Vermont Center for Cardiovascular and Brain Health, University of Vermont, Burlington, VT, USA; [3] Department of Physiology, School of Medicine, University of Maryland, Baltimore, MD, USA; [4] Laboratory of Neurovascular Interactions, Center for Biomedical Engineering and Technology, School of Medicine, University of Maryland, Baltimore, MD, USA; [5] Department of Neurological Sciences, Larner College of Medicine, University of Vermont, Burlington, VT, USA; [6] Institute of Experimental and Clinical Pharmacology and Toxicology, Center of Brain, Behavior and Metabolism (CBBM), University of Lübeck, Lübeck, Germany; [7] German Research Centre for Cardiovascular Research (DZHK), partner site Hamburg/Lübeck/Kiel, Germany; [8] Center of Functionally Integrative Neuroscience, Department of Clinical Medicine, Aarhus University, Aarhus, 8200, Denmark

# These authors contributed equally: Xin Rui Lim, Mohammad M. Abd-Alhaseeb

* Corresponding author: Osama F. Harraz, PhD Osama.Harraz@uvm.edu

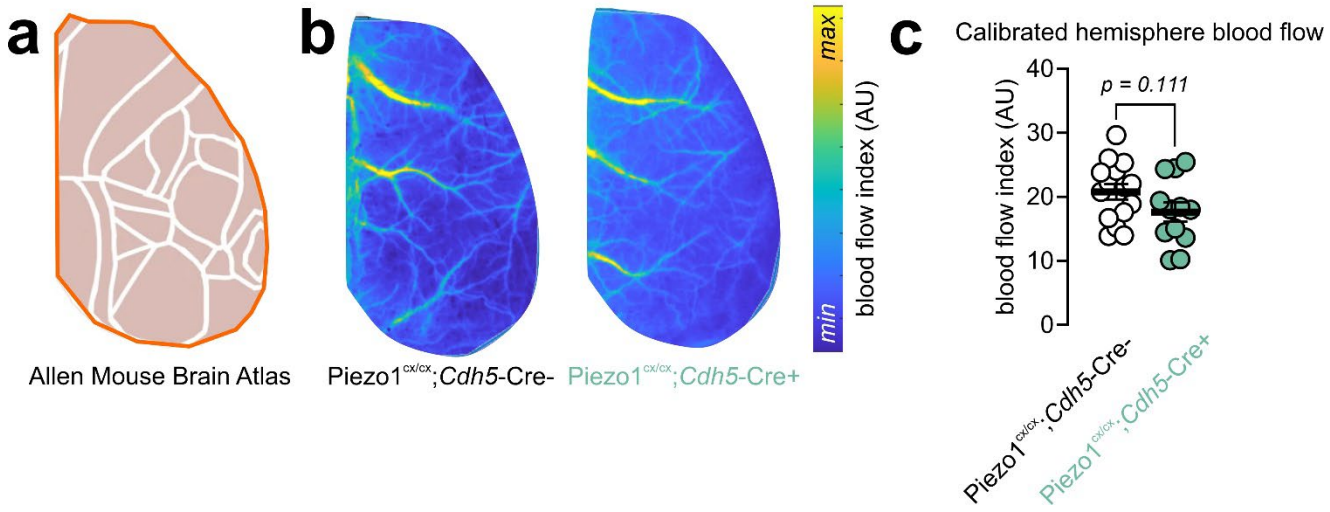

Suppl. Fig. 1. Baseline blood flow in Piezo1$^{cx/cx}$;Cdh5-Cre+ (GOF) mice.

(**a**) Allen mouse brain atlas showing one hemisphere. (**b**) Representative baseline CBF measurements from a control and a Piezo1$^{cx/cx}$;*Cdh5*-Cre+ mouse using LSCI through thinned skulls along with the color scale. (**c**) Calibrated hemisphere blood flow in control (n=13) and Piezo1$^{cx/cx}$;*Cdh5*-Cre+ (n=12) mice (unpaired Student's t test, two-sided). Error bars are standard error of the mean (SEM), data in c are presented as mean ± SEM.

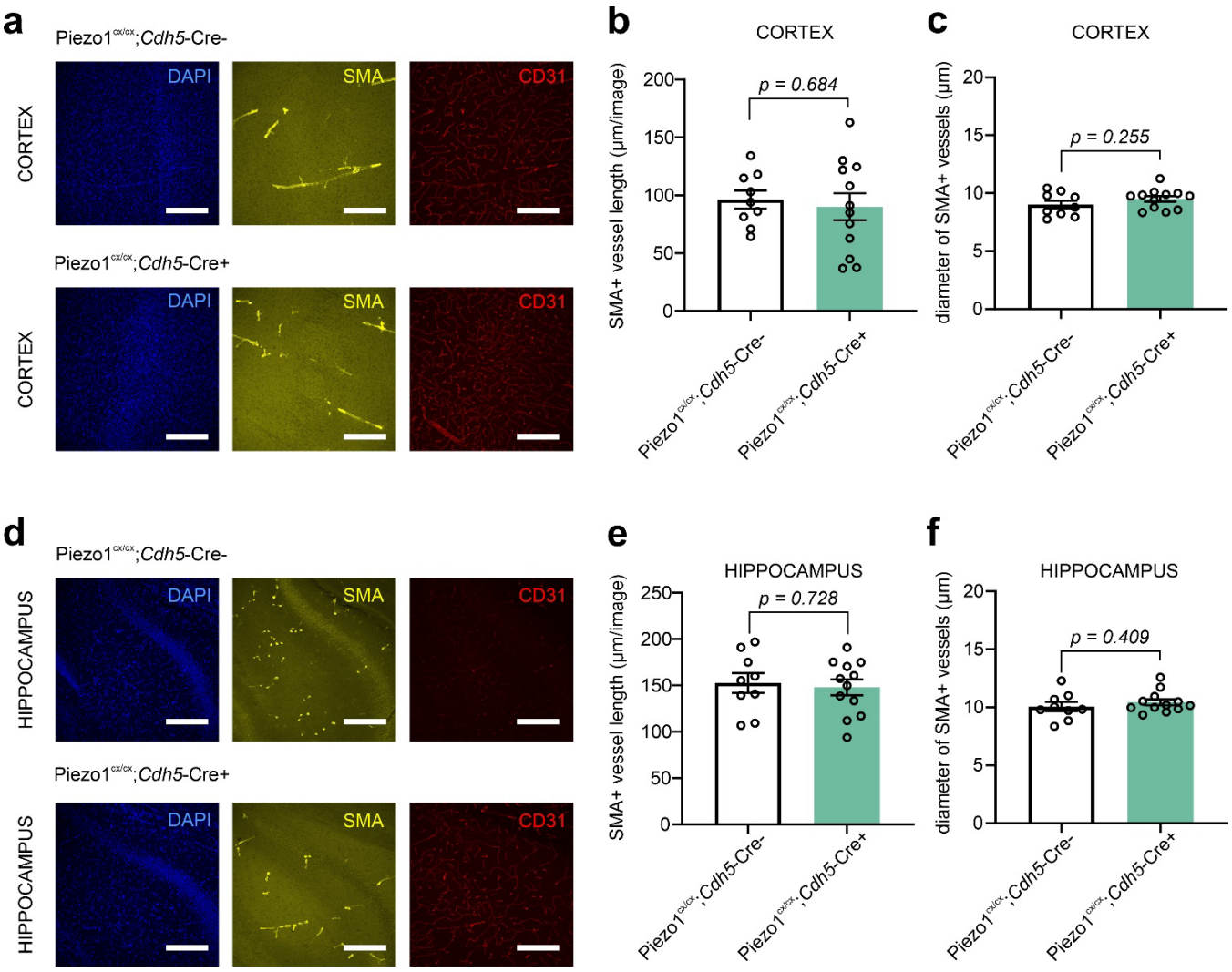

Suppl. Fig. 2. Piezo1$^{cx/cx}$;Cdh5-Cre+ mice show no alteration in arteriolar density or diameter.

(**a**) Exemplary images of staining for arterioles (α-smooth muscle actin, SMA), endothelial cells (CD31), and cell nuclei (DAPI) in cortical brain sections. (**b**) Quantification of the cortical SMA-positive vessel length of Piezo1$^{cx/cx}$;*Cdh5*-Cre+ and control mice. (**c**) Quantification of the mean diameter of cortical SMA-positive vessels of Piezo1$^{cx/cx}$;*Cdh5*-Cre+ and control mice. (**d**) Exemplary staining for SMA, CD31, and DAPI in hippocampal brain sections. (**e**) Quantification of the hippocampal SMA-positive vessel length of Piezo1$^{cx/cx}$;*Cdh5*-Cre+ and control mice. (**f**) Quantification of the mean diameter of hippocampal SMA-positive vessels. All panels: n=9 control, 12 Piezo1$^{cx/cx}$;*Cdh5*-Cre+ mice; unpaired Student's t test (two-sided); scale bars: 200 µm. Error bars are standard error of the mean (SEM), all data are presented as mean ± SEM.

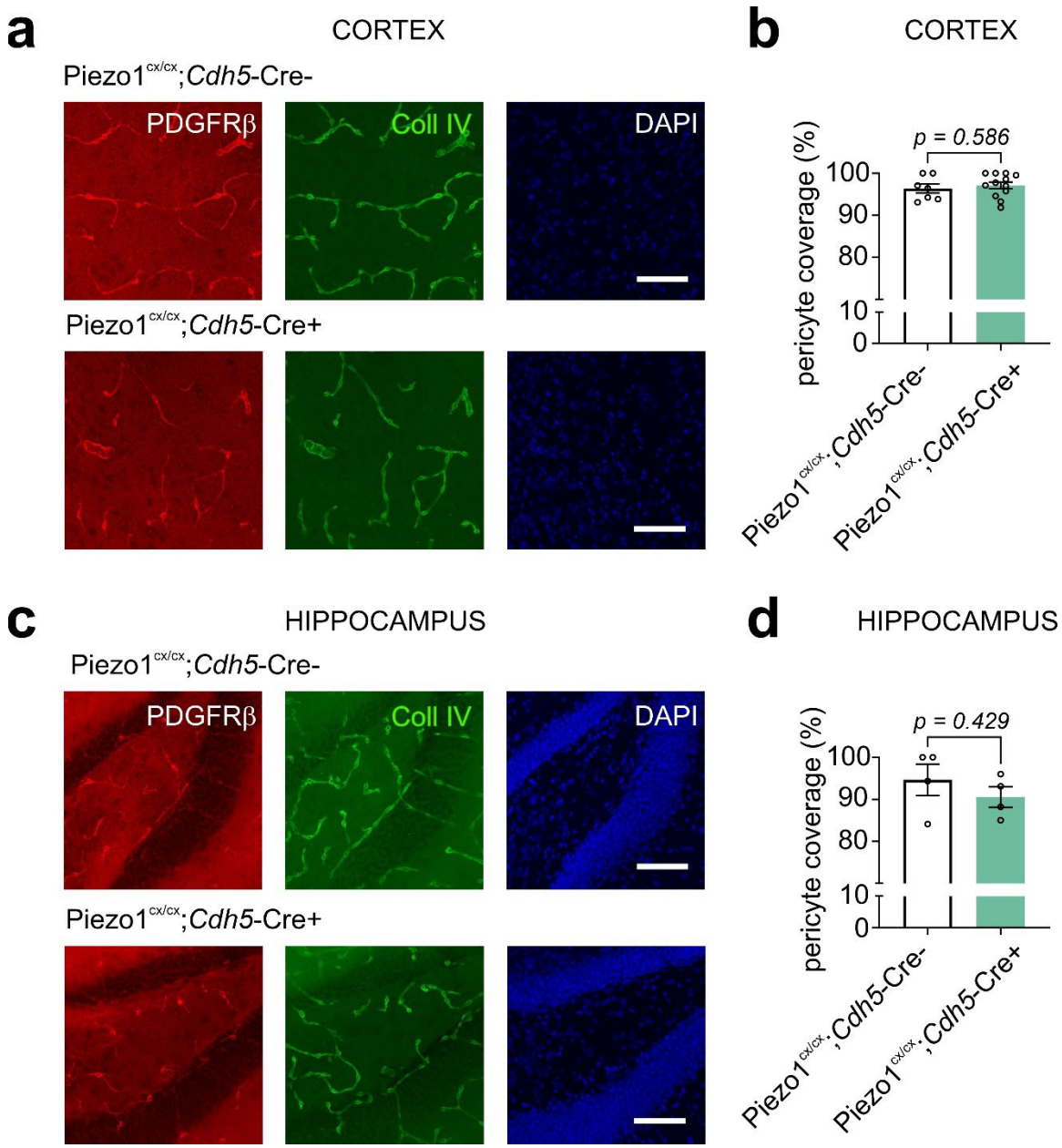

Suppl. Fig. 3. Piezo1$^{cx/cx}$;Cdh5-Cre+ mice show no alteration in pericyte coverage.

(**a**) Exemplary images of staining for the pericyte marker PDGFRβ, basement membranes (collagen IV), and nuclei (DAPI) in cortical brain sections. (**b**) Quantification of the cortical pericyte coverage (calculated as PDGFRβ-positive segments within collagen IV-positive vessels) of Piezo1$^{cx/cx}$;*Cdh5*-Cre+ (n=12) and control (n=7) mice (unpaired Student's t test, two-sided). (**c**) Exemplary staining for PDGFRβ, collagen IV, and DAPI in hippocampal brain sections. (**d**) Quantification of the hippocampal pericyte coverage in Piezo1$^{cx/cx}$;*Cdh5*-Cre+ and control mice (n=4 each; Mann-Whitney test). Scale bars: 200 µm. Error bars are standard error of the mean (SEM), all data are presented as mean ± SEM.

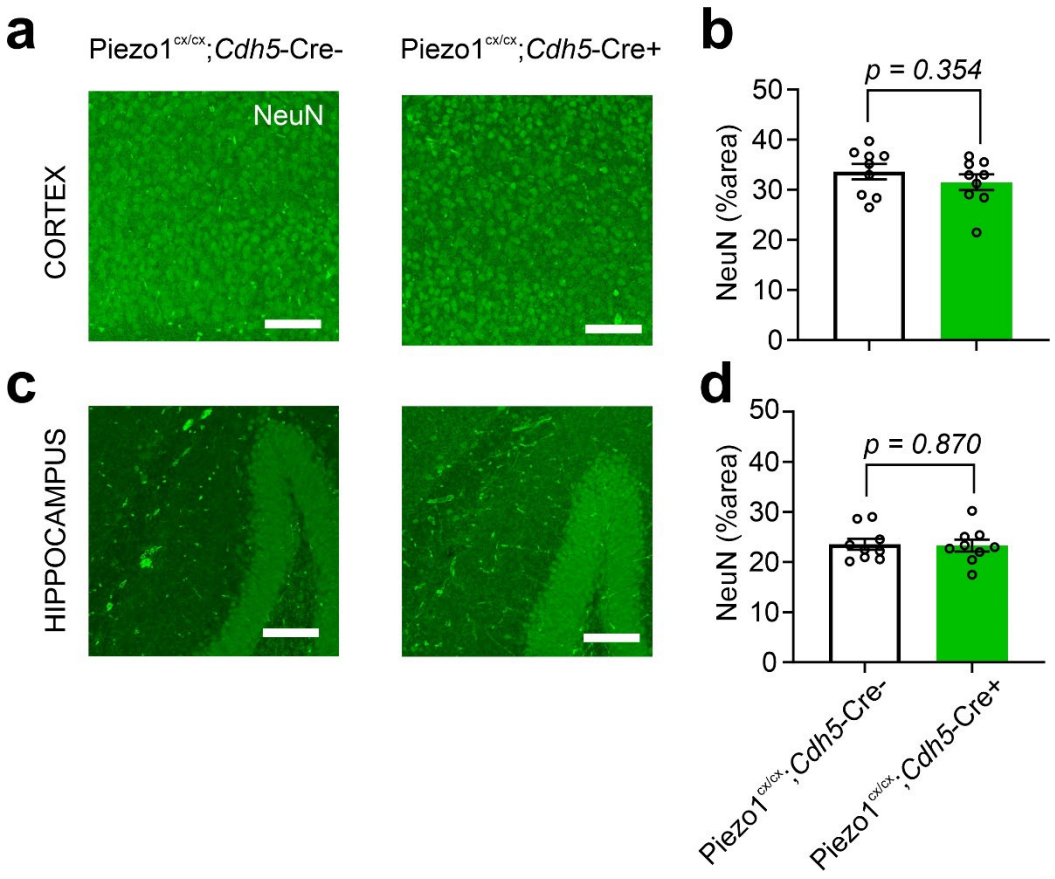

Suppl. Fig. 4. Piezo1$^{cx/cx}$;Cdh5-Cre+ mice demonstrate no difference in neuronal density.

(**a**) Exemplary images of staining for neurons (NeuN) in cortical brain sections. (**b**) Quantification of the cortical NeuN-positive area in Piezo1$^{cx/cx}$;*Cdh5*-Cre+ and control mice. (**c**) Exemplary images of NeuN staining in hippocampal brain sections. (**d**) Quantification of the hippocampal NeuN-positive area. All panels: n=9 control, 9 Piezo1$^{cx/cx}$;*Cdh5*-Cre+ mice; unpaired Student's t test (two-sided); scale bars: 100 µm. Error bars are standard error of the mean (SEM), all data are presented as mean ± SEM.

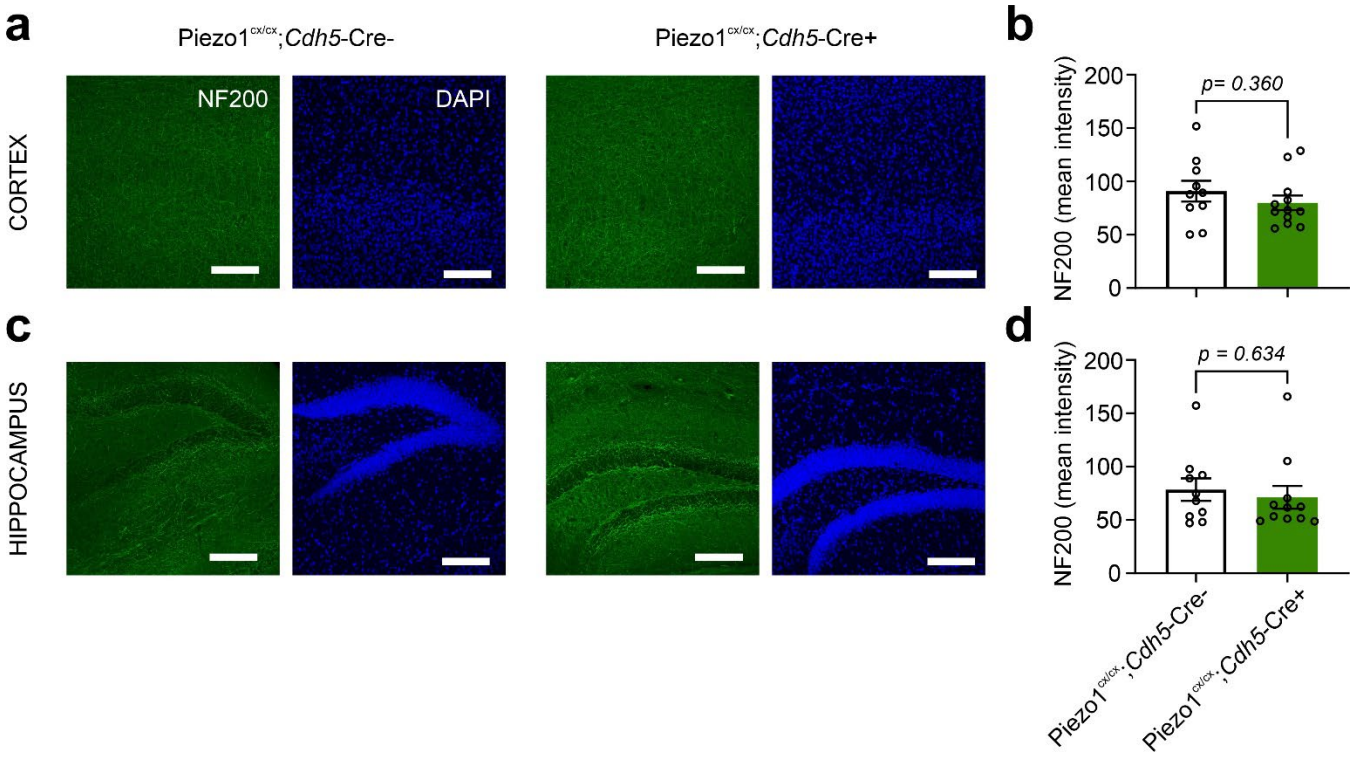

Suppl. Fig. 5. Piezo1$^{cx/cx}$;Cdh5-Cre+ mice demonstrate no difference in the mean intensity of the neuronal marker neurofilament 200 (NF200).

(**a**) Exemplary images of staining for neurons (NF200, green) and nuclei (DAPI, blue) in cortical brain sections. (**b**) Quantification of the mean intensity of NF200 staining in Piezo1$^{cx/cx}$;*Cdh5*-Cre+ (n=12) and control (n=10) mice. (**c**) Exemplary images of NF200 staining in hippocampal brain sections. (**d**) Quantification of the hippocampal NF200 staining (n=10 control, n=11 Piezo1$^{cx/cx}$;*Cdh5*-Cre+ mice; unpaired Student's t test (two-sided); scale bars: 200 µm). Error bars are standard error of the mean (SEM), all data are presented as mean ± SEM.

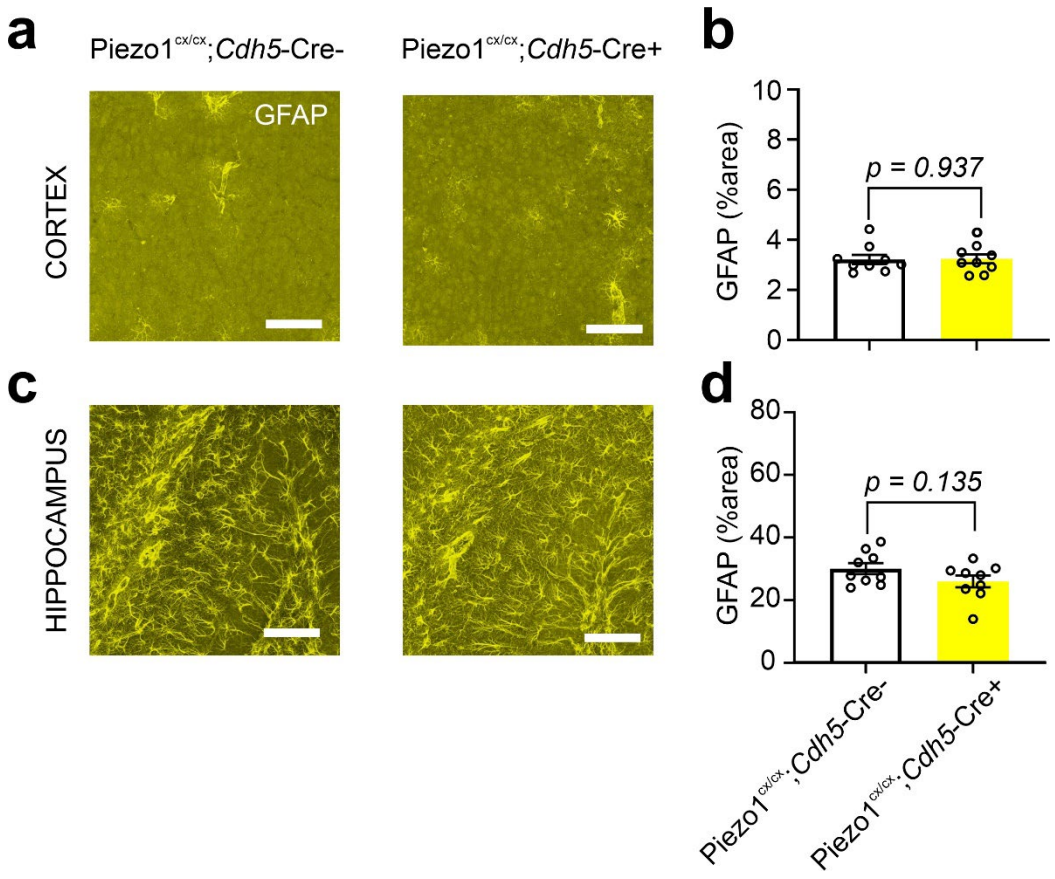

Suppl. Fig. 6. Piezo1$^{cx/cx}$;Cdh5-Cre+ mice show no alteration in astrocyte activation marker.

(**a**) Exemplary images of staining for activated astrocytes (GFAP) in cortical brain sections. (**b**) Quantification of the cortical GFAP-positive area of Piezo1$^{cx/cx}$;*Cdh5*-Cre+ and control mice. (**c**) Exemplary images of GFAP staining in hippocampal brain sections. (**d**) Quantification of the hippocampal GFAP-positive area. All panels: n=9 control, 9 Piezo1$^{cx/cx}$;*Cdh5*-Cre+ mice; unpaired Student's t test (two-sided); scale bars: 100 µm. Error bars are standard error of the mean (SEM), all data are presented as mean ± SEM.

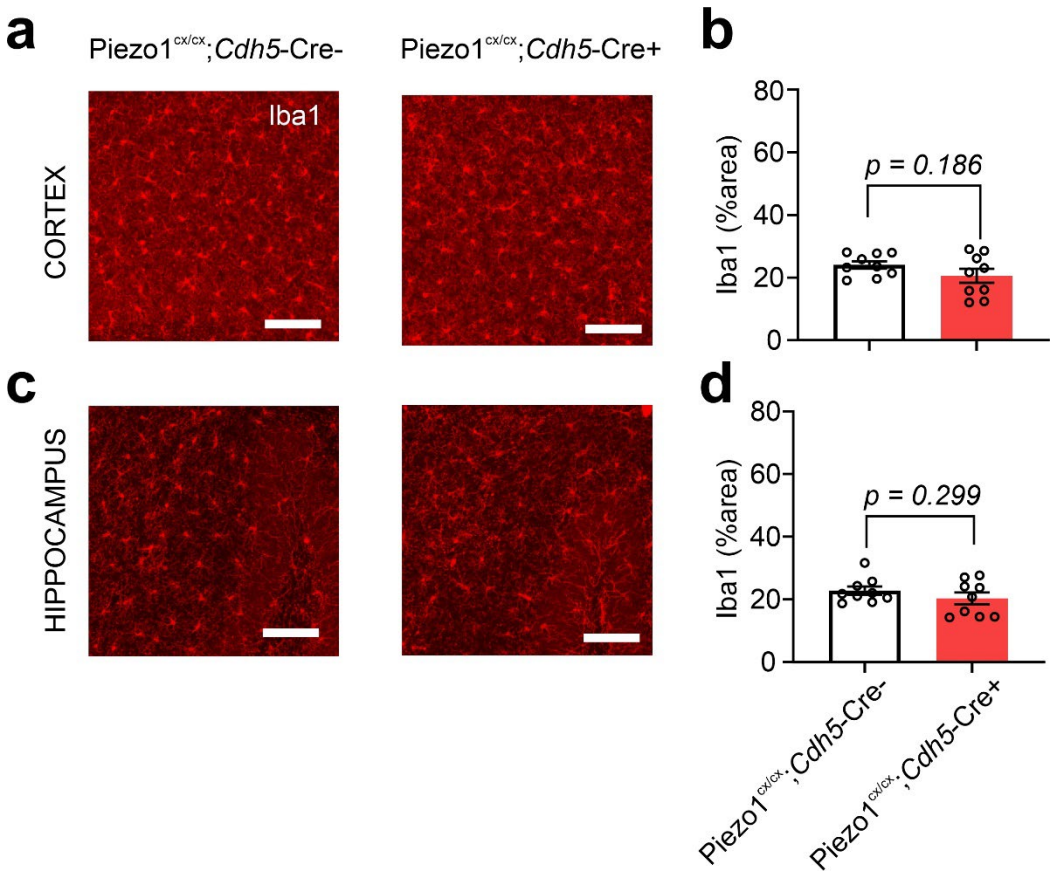

Suppl. Fig. 7. Piezo1$^{cx/cx}$;Cdh5-Cre+ mice show no change in microglia density.

(**a**) Exemplary images of staining for microglia (Iba1) in cortical brain sections. (**b**) Quantification of the cortical Iba1-positive area of Piezo1$^{cx/cx}$;*Cdh5*-Cre+ and control mice. (**c**) Exemplary images of staining for Iba1 in hippocampal brain sections. (**d**) Quantification of the hippocampal Iba1-positive area. All panels: n=9 control, 9 Piezo1$^{cx/cx}$;*Cdh5*-Cre+ mice; unpaired Student's t test (two-sided); scale bars: 100 µm. Error bars are standard error of the mean (SEM), all data are presented as mean ± SEM.

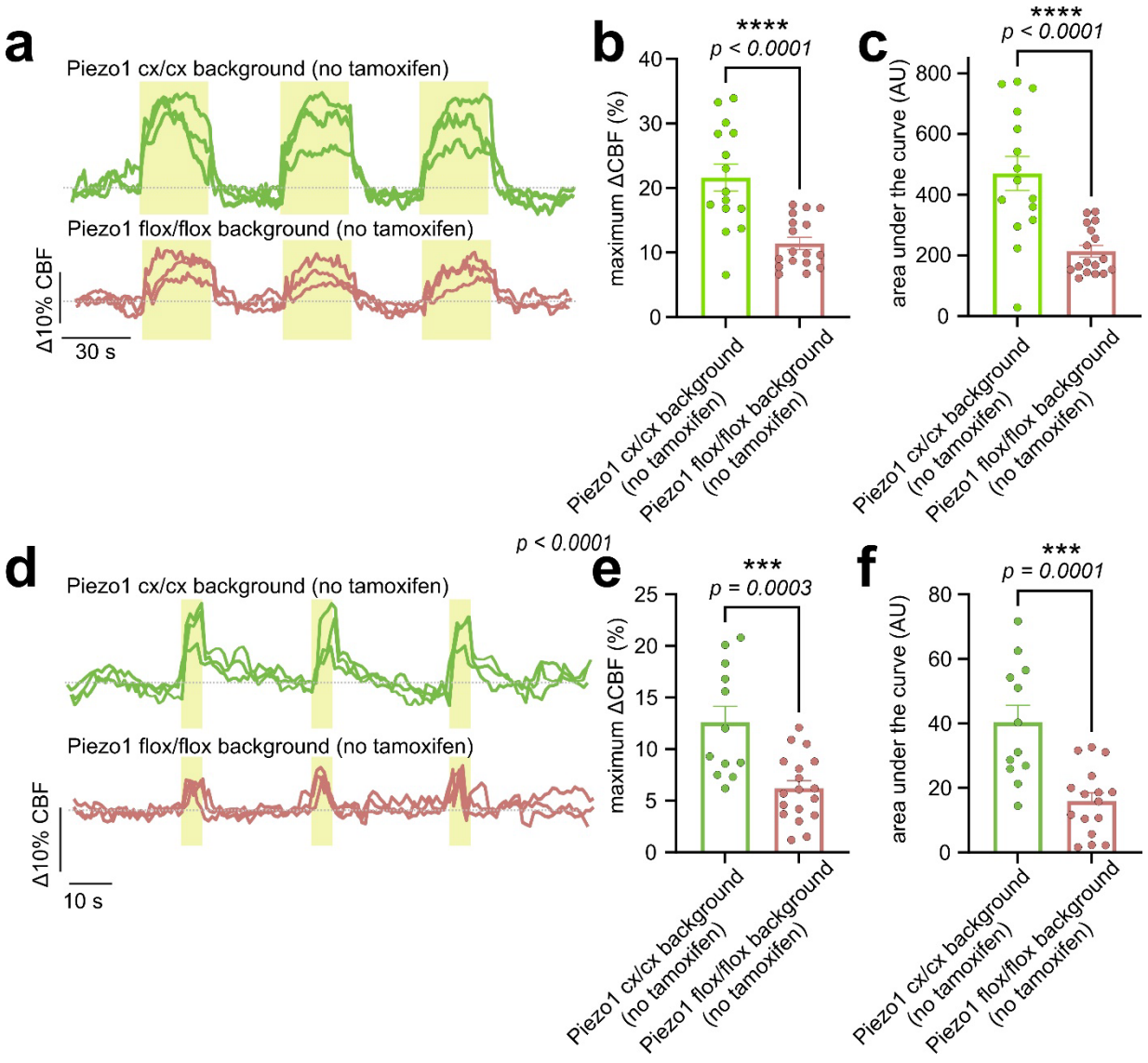

Suppl. Fig. 8. Genetic backgrounds of Piezo1$^{cx/cx}$ and Piezo1$^{flox/flox}$ mice affect FH.

(**a**) Representative traces of blood flow index measured using LSCI in anesthetized mice undergoing whisker stimulation (air puff, 30 s, 5 Hz). All mice (n=4) received no tamoxifen. Both Cre+ and Cre- mice were used, and data were grouped based on whether the mice were homozygous floxed Piezo1 (Piezo1$^{flox/flox}$) or floxed knock-in mutant mice (Piezo1$^{cx/cx}$). (**b, c**) Whisker stimulation evoked varying magnitude changes in CBF in mice of different backgrounds. (**d**) Similar to *a* but using 5-s stimulations. (**e, f**) Mice of Piezo1$^{flox/flox}$ background demonstrated reduced responses to whisker stimulation. Unpaired Student t-tests were used (two-sided, ***$p < 0.001$, ****$p < 0.0001$). Error bars are standard error of the mean (SEM), all data are presented as mean ± SEM.

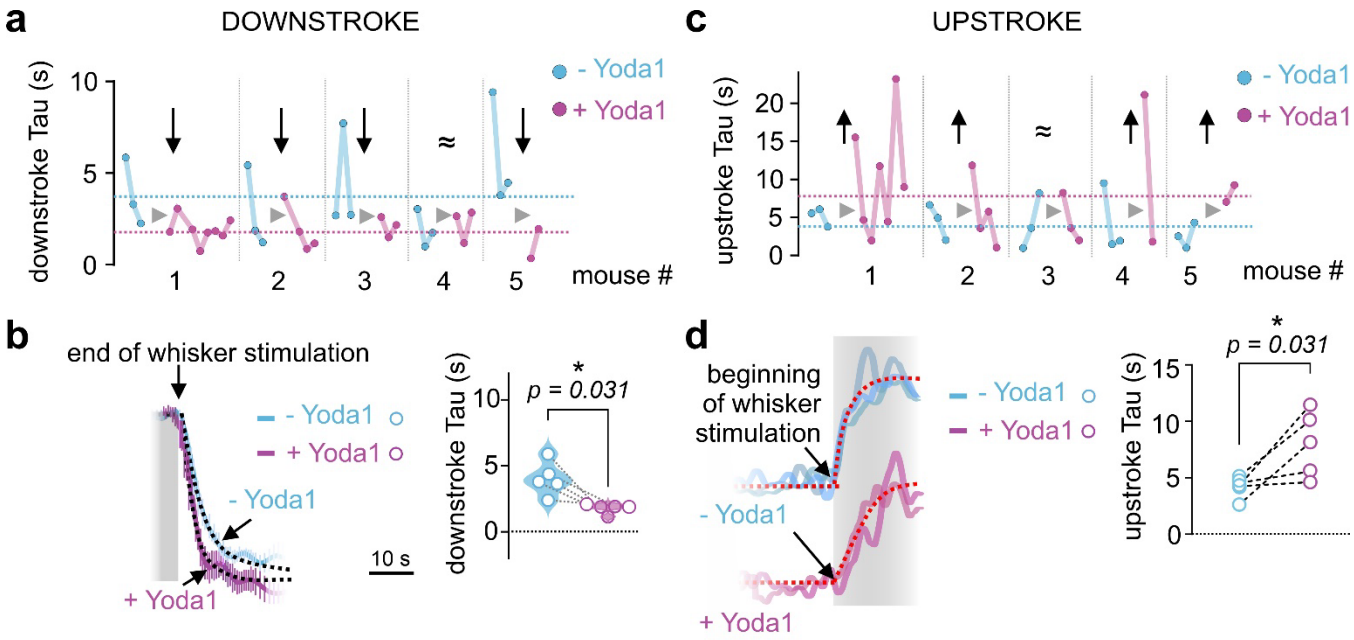

Suppl. Fig. 9. FH kinetics change after pharmacological Piezo1 activation.

(**a**) Time constants of the downstroke phase of CBF in response to whisker stimulation. CBF was assessed using laser Doppler flowmetry through a cranial window in 5 C57BL/6J mice before and after Yoda1 (30 µM, cortical) application. (**b**) Averaged traces and fittings to obtain downstroke Tau in the absence or presence of Yoda1 (n= 5 mice). (**c**) Time constants of FH upstroke in 5 mice before and after Yoda1. (**d**) Representative traces and fittings of FH upstroke. Arrows in *a* and *c* denote decrease or increase and ≈ denotes no change (n= 5 mice). Wilcoxon test was used (*$P < 0.05$).

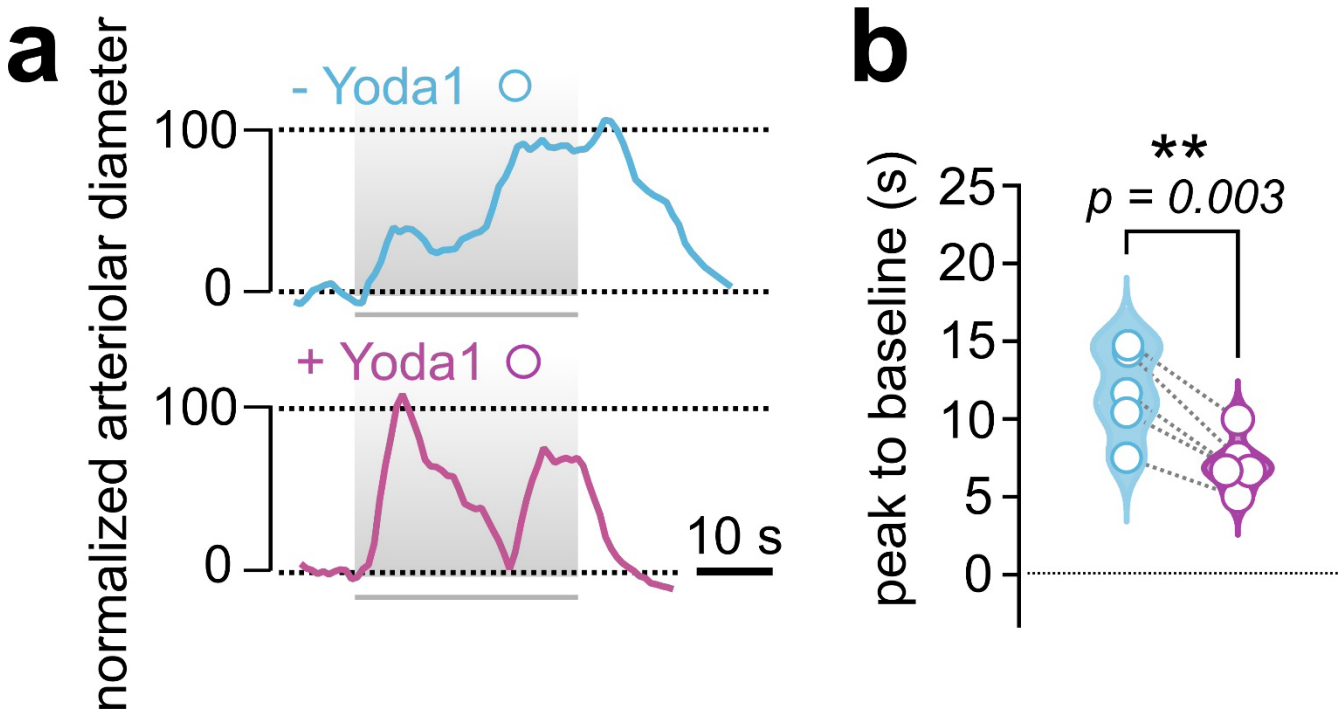

Suppl. Fig. 10. Arteriolar dilation kinetics are altered after pharmacological Piezo1 activation.

(**a**) Representative normalized traces showing the effects of Yoda1 on penetrating arteriolar diameter and its return to baseline after whisker stimulation. (**b**) Time from peak diameter to baseline was calculated in the absence and presence of 30 µM Yoda1 (n=5 mice, paired Student t-test, two-sided, $^{**}P < 0.01$). Arteriolar diameter responses were measured through a cranial window using two-photon microscopy.

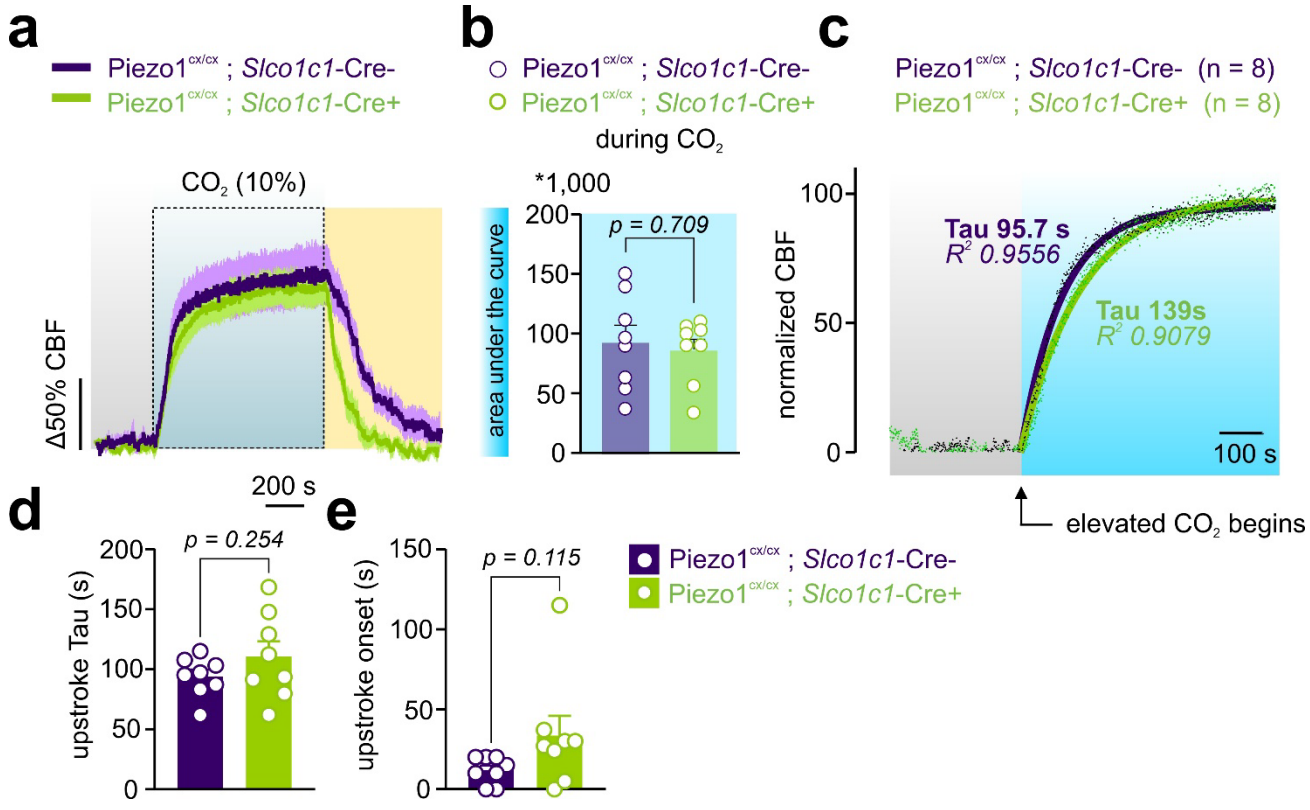

Suppl. Fig. 11. CO_2-induced hyperemia in Piezo1$^{cx/cx}$;Slco1c1-Cre+ mice.

(**a**) Averaged changes in CBF in control (*purple*) and Piezo1$^{cx/cx}$;*Slco1c1*-Cre+ (*green*) mice (n=8 mice/group). (**b**) Areas under the curve during CO_2 elevation (15-min) demonstrate comparable CBF increases (n=8 mice each). (**c**) Normalized averaged CBF increases to hypercapnia from control and GOF mice. The bold lines show the exponential fittings of the upstroke phase along with the time constants (Tau). (**d, e**) Scatter plots of upstroke Tau and onset (lag) from Piezo1$^{cx/cx}$;*Slco1c1*-Cre+ and control mice (n=8 mice each). All statistical tests were unpaired Student's *t* test (two-sided). Error bars are standard error of the mean (SEM), all data are presented as mean ± SEM.

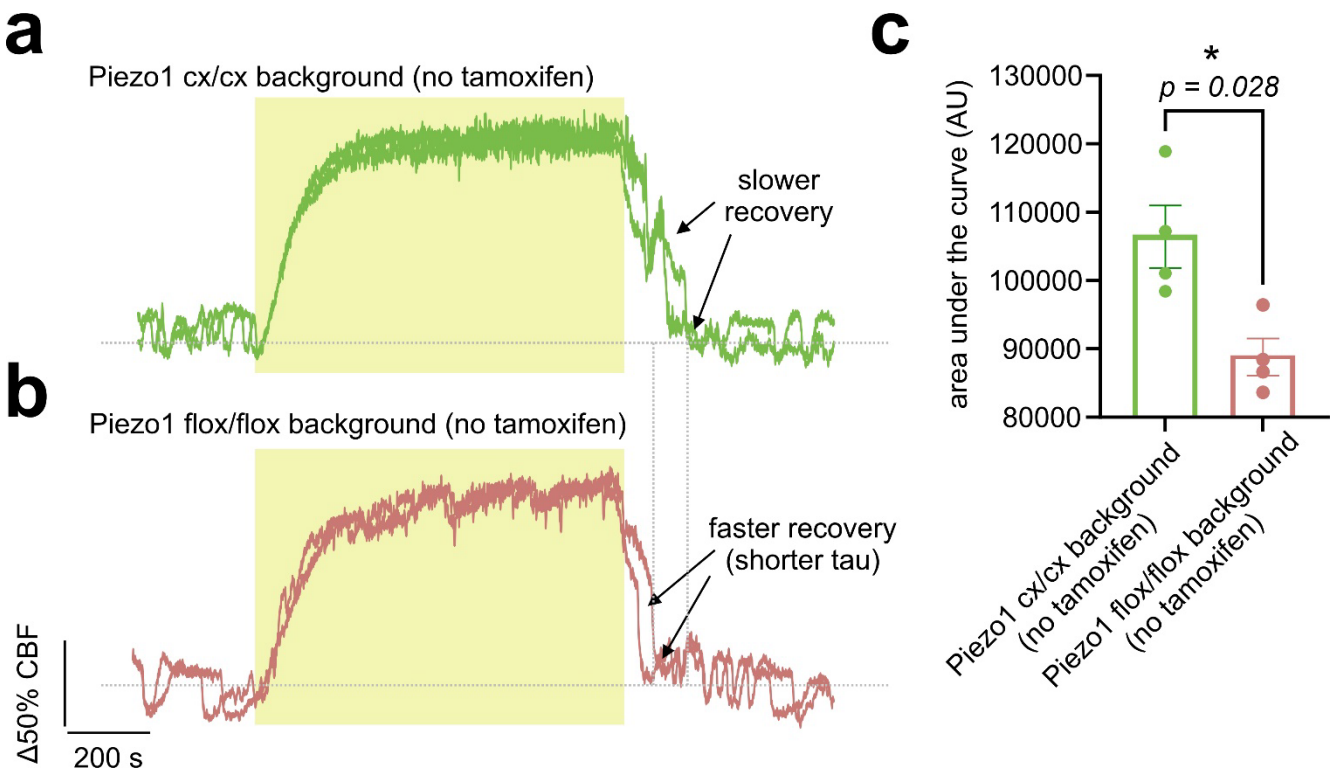

Suppl. Fig. 12. Genetic backgrounds of Piezo1$^{cx/cx}$ and Piezo1$^{flox/flox}$ mice affect CO_2-induced hyperemia.

(**a, b**) Representative traces of blood flow index measured using LSCI in anesthetized mice undergoing hypercapnia stimulation (10% CO_2 inhalation for 15 min, yellow background). All mice received no tamoxifen (n=4). Both *Slco1c1*-Cre+ and *Slco1c1*-Cre- mice were used, where data are presented based on whether the mice were on a Piezo1$^{cx/cx}$ (*a*) or a Piezo1$^{flox/flox}$ (*b*) background. (**c**) Area under the curve analyses of CO_2-evoked changes in CBF in mice of different backgrounds (Mann-Whitney test, $*p < 0.05$). Error bars are standard error of the mean (SEM), data are presented as mean ± SEM.

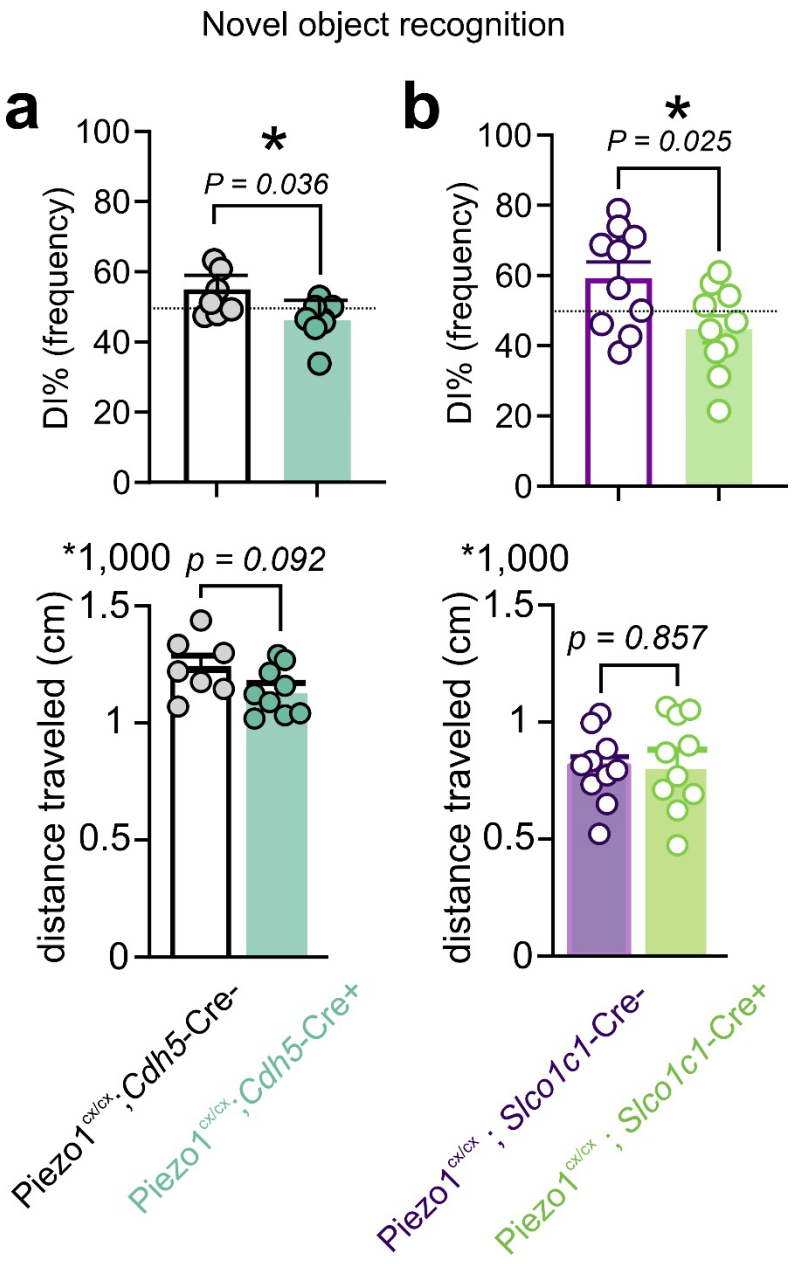

Suppl. Fig. 13. Piezo1 GOF leads to memory impairments.

Discrimination index (DI%, frequency) for the NOR test was calculated using the number of times the mouse interacted with the objects and the distances traveled throughout the test. Piezo1$^{cx/cx}$;*Cdh5*-Cre+ (*a*) and Piezo1$^{cx/cx}$;*Slco1c1*-Cre+ (*b*) mice had lower DI compared to their controls (n=7, 9, 10 mice per genotype, unpaired Student's t test, two-sided, *P > 0.05). There was no change in locomotor activity. Error bars are standard error of the mean (SEM), data are presented as mean ± SEM.

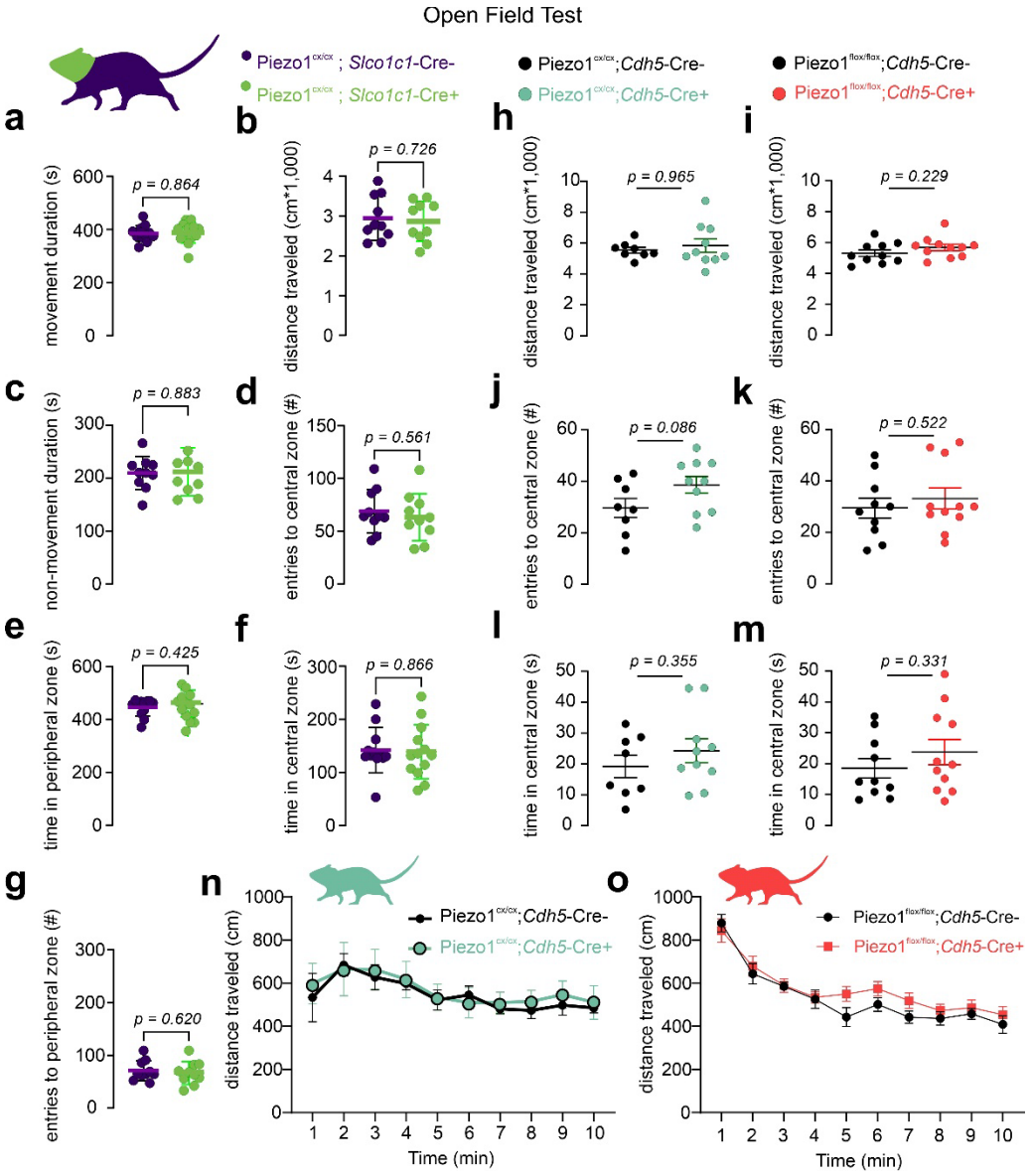

Suppl. Fig. 14. Open field test in mice with genetically altered endothelial Piezo1 function.

(**a-g**) Different parameters assessed during the open field test in Piezo1$^{cx/cx}$;*Slco1c1*-Cre+ and control mice over 600 s (n=10 mice per genotype). Parameters included total movement and non-movement durations (*a, c*), total distance traveled (*b*), time spent in central and peripheral zones (e, f), and entries to central and peripheral zones (*d, g*). (**h-m**) Open field test results from Piezo1$^{cx/cx}$;*Cdh5*-Cre+ (n=8) and control (n=10) mice (*h, j, l*), and Piezo1$^{flox/flox}$;*Cdh5*-Cre+ (n=11) and control (n=10) mice (*i, k, m*). Comparisons in *a-m* are unpaired Student's t test (two-sided). (**n**) Binned traveled distances during the open field test in Piezo1$^{cx/cx}$;*Cdh5*-Cre+ (n=8) and control mice (n=7). A main effect of time [$F(2.5, 22.1)=4.0$, $P=0.026$] demonstrates decreased locomotion throughout the open field tests, consistent with habituation to the novel environment. (**o**) Decreased locomotion throughout the open field test in Piezo1$^{flox/flox}$;*Cdh5*-Cre+ and controls mice [$F(3.4,36.9=34.6$, $P<0.001$] is consistent with habituation to the novel environment. Error bars are standard error of the mean (SEM), data are presented as mean ± SEM.

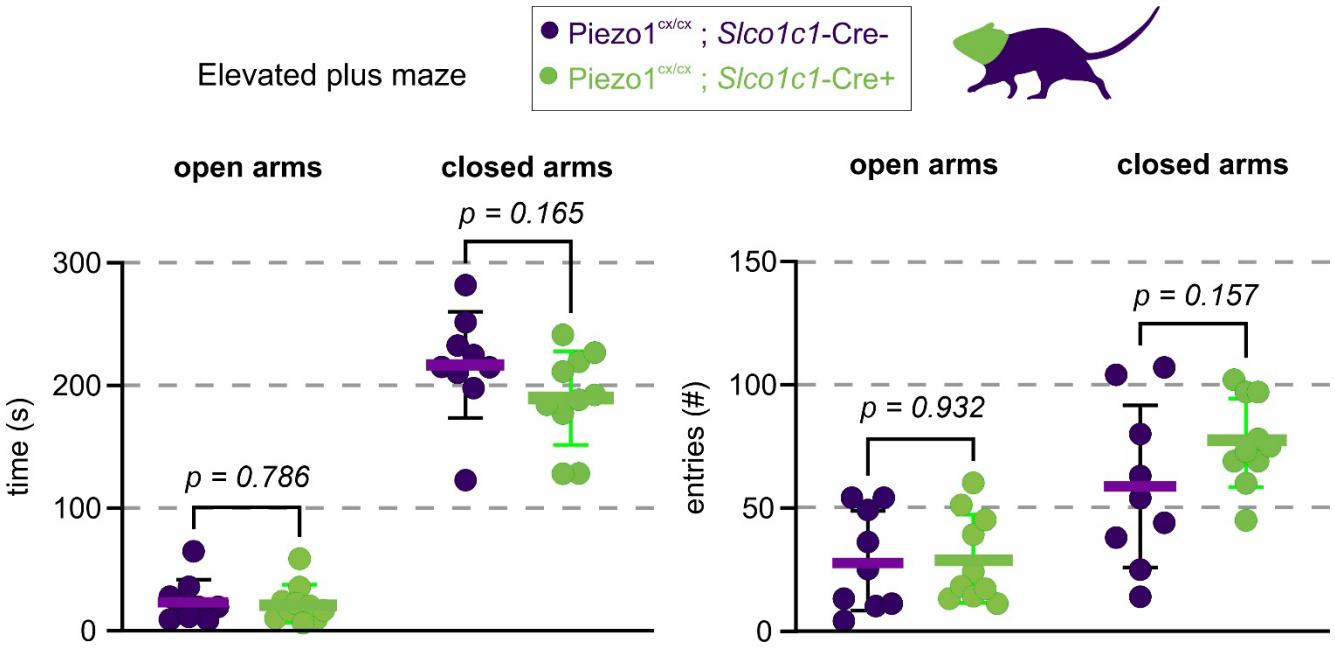

Suppl. Fig. 15. Elevated plus maze test in Piezo1$^{cx/cx}$;Slco1c1-Cre+ mice.

Time spent in the open and closed arms and the number of entries to each arm of the elevated plus maze setup (n=9 control, 10 Piezo1$^{cx/cx}$;*Slco1c1*-Cre+ mice; unpaired Student's *t* test, two-sided). Error bars are standard error of the mean (SEM), data are presented as mean ± SEM.

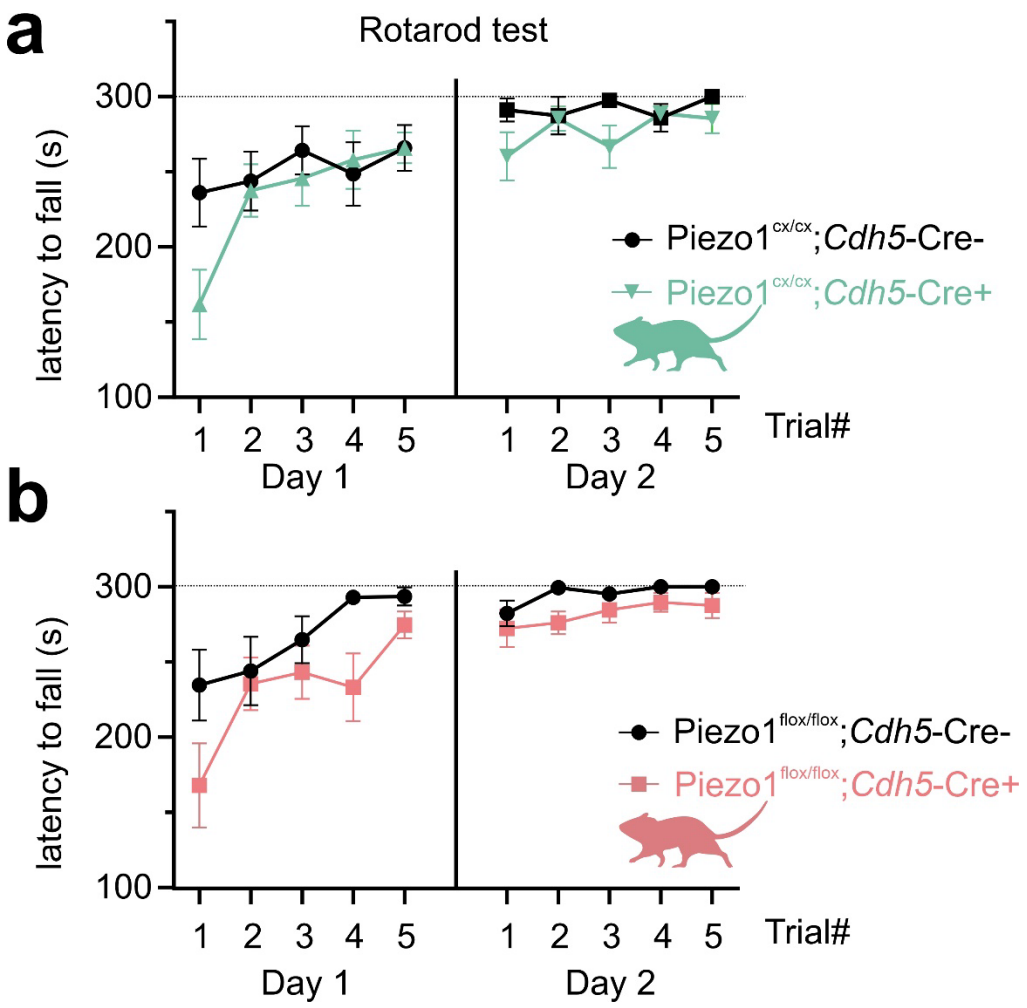

Suppl. Fig. 16. Rotarod test in endothelial Piezo1 gain-of-function and knockout mice.

(**a**) Latency to fall during a 5-min rotarod test in control (n=11) and Piezo1$^{cx/cx}$;*Cdh5*-Cre+ (n=14) mice. The test was performed over two consecutive days, with 5 trials on each day. (**b**) Similar to *a* but in control (n=11) and Piezo1$^{flox/flox}$;*Cdh5*-Cre+ mice (n=10). On Day 1, a main effect of Time indicated improved performance indicative of motor learning in the Piezo1$^{cx/cx}$;*Cdh5*-Cre+ [$F(3.3, 75.8)=6.9$, $P<0.001$] and Piezo1$^{flox/flox}$;*Cdh5*-Cre+ mice [$F(2.6, 49.1)=7.6$, $P=0.001$] and their respective controls. A Time x Genotype interaction in the Piezo1$^{cx/cx}$;*Cdh5*-Cre+ [$F(4,92) = 2.8$, $P=0.031$] suggests a mild impairment and early deficit in rotarod performance that recovers, showing similar asymptotic motor learning to controls. Similarly, a main effect of Genotype in the Piezo1$^{flox/flox}$;*Cdh5*-Cre+ [$F(1,19)=4.6$, $P=0.046$] implicates that while they showed motor learning, there was a mild deficit in rotarod performance. No differences between either genotype or their controls were observed on Day 2, suggesting that any impairment on Day 1 was not due to a gross motor deficit. Error bars are standard error of the mean (SEM), data are presented as mean ± SEM.

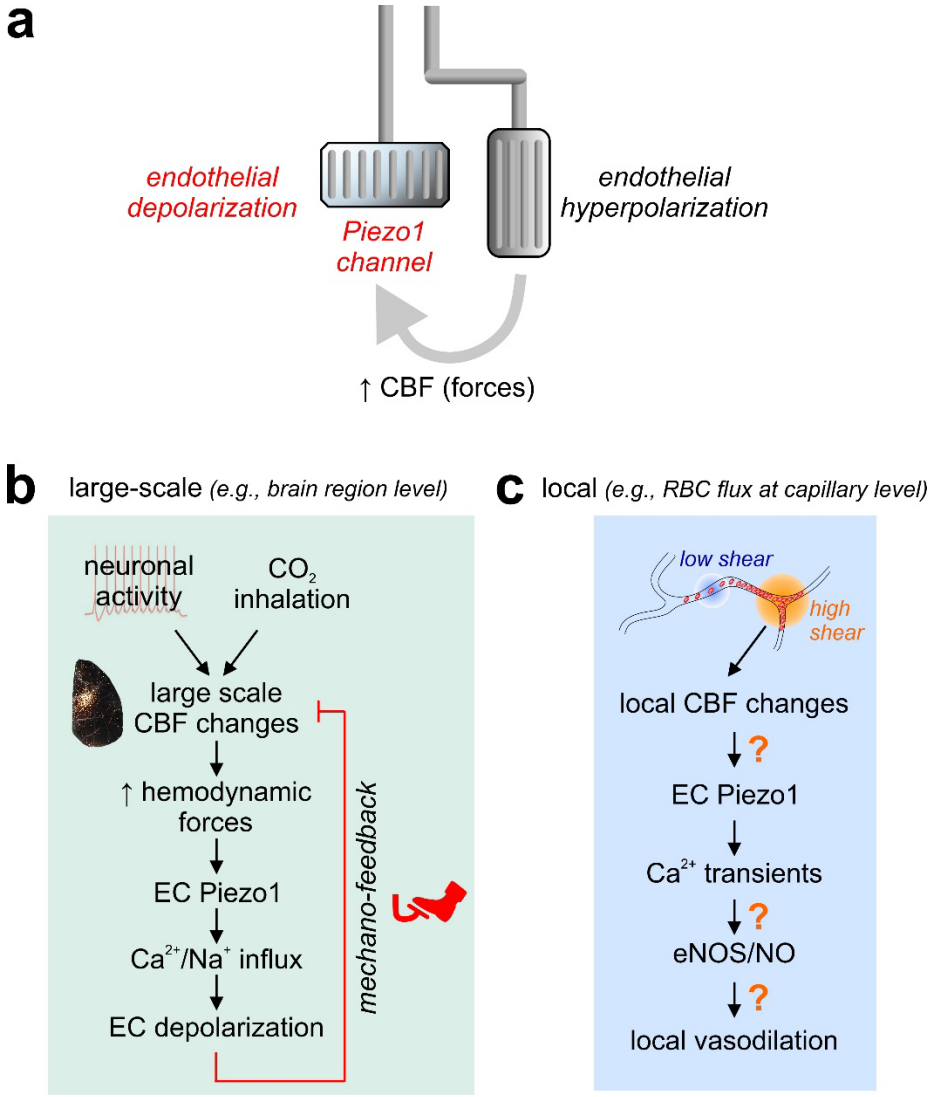

Suppl. Fig. 17. Proposed mechanism by which brain endothelial Piezo1 regulates CBF.

(**a**) Schematic illustrating that endothelial hyperpolarization in response to neural activity leads to hyperemia (↑CBF), which in turn engages Piezo1 as a brake system. (**b**) Large-scale changes in CBF in a brain region (e.g., somatosensory cortex) trigger major hemodynamic forces on cerebrovascular ECs throughout the vascular tree (arteries, arterioles, capillaries, venules and veins). Forces activate Piezo1 channels, thus resetting the membrane potential and acting as a built-in brake system that facilitates blood flow recovery to baseline. (**c**) At the local level (e.g., capillaries), spatially restricted changes in blood flow could act as a trigger for endothelial Piezo1 channels. The latter leads to Ca^{2+} signaling in ECs and NO generation, which causes local vasodilation in areas of high shear stress. Question marks denote unknown signaling steps.